A novel adaptive particle swarm optimization algorithm based high precision parameter identification and state estimation of lithium-ion battery.

HE, M., WANG, S., FERNANDEZ, C., YU, C., LI, X. and BOBOBEE, E.D.

2021

Int. J. Electrochem. Sci., 16 **(2021)** Article ID: 21054, doi: 10.20964/2021.05.55

International Journal of
ELECTROCHEMICAL
SCIENCE
www.electrochemsci.org

A Novel Adaptive Particle Swarm Optimization Algorithm Based High Precision Parameter Identification and State Estimation of Lithium-Ion Battery

Mingfang He[1], *Shunli Wang*[1,*], *Carlos Fernandez*[2], *Chunmei Yu*[1], *Xiaoxia Li*[1], *Etse Dablu Bobobee*[1]

[1] School of Information Engineering, Southwest University of Science and Technology, Mianyang 621010, China;
[2] School of Pharmacy and Life Sciences, Robert Gordon University, Aberdeen AB10-7GJ, UK.
[*]E-mail: 497420789@qq.com

Received: 18 November 2020 / *Accepted:* 12 January 2021 / *Published:* 31 March 2021

Lithium-ion batteries are widely used in new energy vehicles, energy storage systems, aerospace and other fields because of their high energy density, long cycle life and high-cost performance. Accurate equivalent modeling, adaptive internal state characterization and accurate state of charge estimation are the cornerstones of expanding the application market of lithium-ion batteries. According to the highly nonlinear operating characteristics of lithium-ion batteries, the Thevenin equivalent model is used to characterize the operating characteristics of lithium-ion batteries, particle swarm optimization algorithm is used to process the measured data, and adaptive optimization strategy is added to improve the global search ability of particles, and the parameters of the model are identified innovatively. Combined with extended Kalman algorithm and Sage-Husa filtering algorithm, the state-of-charge estimation model of lithium ion battery is constructed. aiming at the influence of fixed and inaccurate noise initial value in traditional Kalman filtering algorithm on SOC estimation results, Sage-Husa algorithm is used to adaptively correct system noise. The experimental results under HPPC condition show that the maximum error of the model is less than 1.5%. Simulation results of SOC estimation algorithm under two different operating conditions show that the maximum estimation error of adaptive extended Kalman algorithm is less than 0.05, which realizes high-precision lithium battery model parameter identification and high-precision state-of-charge estimation.

Keywords: Lithium-ion battery, Adaptive particle swarm optimization, Sage-Husa algorithm, Adaptive extended Kalman filter, State of charge estimation

1. INTRODUCTION

With the increasing emphasis on environmental resources in the world, green and safe new energy is gradually entering the public's field of vision. Among them, lithium-ion batteries have been

widely used in high-end emerging industries such as new energy vehicles, aerospace, rail transit, etc. due to their advantages of high specific energy, high-cost performance, and long cycle life[1]. Lithium batteries are growing at an annual rate of more than 50%, Promoting the transformation of the modern energy landscape[2, 3]. Under the background of increasing market demand for lithium-ion batteries and the gradual expansion of application fields, the safe and reliable operation of lithium-ion batteries has become a key issue that needs to be broken through.

The Lithium battery is a system with highly nonlinear operating characteristics. The acquisition and modeling of its internal time-varying parameters are important factors that affect the accurate characterization and accurate state of charge estimation of lithium-ion batteries[4, 5]. To effectively establish the state space expression of lithium batteries, an equivalent model with high adaptability must be established[6, 7]. According to different modeling mechanisms, lithium battery equivalent models can be divided into electrochemical models, intelligent mathematical models, and equivalent circuit models[8]. The electrochemical model can accurately characterize the working characteristics of lithium batteries, but the calculation is complex and is not suitable for the battery state detection platform with high real-time requirements[9-12]. The intelligent mathematical model is mainly a neural network model, which can theoretically complete battery modeling[13]. However, due to the need for a large amount of actual data for training, high technical threshold and long processing time, its practical application is limited[14]. The equivalent circuit model can simulate the electrochemical reaction inside the lithium battery through related circuit components. Its calculation is simple and easy to process in real time, so it is widely used at present[15]. Mu et al.combined a lithium battery electrochemical impedance spectroscopy to establish a fractional equivalent circuit model. Ability to better characterize the battery in the low SOC range[16]. Simone et al. added a thermal model to the equivalent circuit model under the premise of considering the influence of external temperature and thermal management on capacity and power attenuation and the possible thermal runaway and package imbalance, thus reducing the influence of environmental factors on the model characterization effect[17].

The state-of-charge (SOC) of lithium-ion battery is an index to describe the remaining capacity of the battery, and it is also one of the most important parameters in the use of the battery[18, 19]. SOC of lithium-ion battery is affected by its internal electrochemical reaction, charge-discharge mechanism and external environmental conditions, including charge-discharge rate, self-discharge, temperature and aging[20-22]. These factors will cause some changes in the residual power, so it is difficult to accurately estimate the SOC of the battery. At present, the SOC estimation methods of lithium-ion batteries mainly include open-circuit voltage method[23], ampere-hour (Ah) integration method, internal resistance method[24], neural network method, Kalman filter (KF) method, particle filter(PF) method, etc. [3, 25, 26].. Open-circuit voltage method uses the one-to-one correspondence between open-circuit voltage and charging state, and obtains the charging state value by obtaining the open-circuit voltage value of the battery, so as to achieve the estimation purpose[27]. Although this method can measure SOC value, it is necessary to let the battery stand for more than one hour before starting measurement. The battery itself is easily affected by temperature and reproduction quality. In the same OCV, the difference of SOC under different conditions is different[28]. Therefore, it is not suitable for SOC estimation in operation. Ampere-hour integration method, also known as current integration method, estimates the state of charge (SOC) of the battery by accumulating the charge and discharge amount of the battery during charging

and discharging, and corrects the state of charge value by charging and discharging rate and battery temperature[13, 29, 30]. This method can not only accurately estimate the state of charge, but also realize real-time estimation[31]. The method is simple and the principle is easy to understand. A single method is not enough. Its shortcomings may have a significant impact on SOC estimation[32]. For example, the essence of ampere-hour integration method is superposition process[33]. If the initial value measurement is not accurate enough, it will cause measurement deviation[34-36]. In addition, when collecting current, the self-discharge effect, aging condition and charge-discharge rate of the battery itself are not considered in the calculation formula[20]. Long-term integration process will accumulate effects, and the error will continue to expand, resulting in SOC deviating from the true value in the estimation process[37]. The neural network method estimates the charging state of lithium ion batteries by processing a large number of real-time input and output data of lithium ion batteries. Kalman filtering method obtains the optimal solution in the sense of minimum variance through continuous iterative operation.

In recent years, a large number of scholars have studied the estimation algorithm of SOCunder the influence of a complex external environment. Chen et al. proposed an on-line estimation method of open circuit voltage based on particle filter, and realized the charge state based on voltage[38]. He et al. established a new unbiased equivalent circuit model to eliminate current bias, and based on the unbiased equivalent circuit model, proposed a two-layer estimator to estimate charge state by using real-time identified model parameters[19]. In this paper, Liu et al. proposed a hybrid model of SOC of lithium-ion battery, which is composed of deep beliefnetwork (DBN) and Kalman filter under dynamic conditions[38]. The researchers of Tsinghua University State Key Laboratory of Automotive Safety and Energy combined the Ah method with low calculation amount and the adaptive extended Kalman filter (AEKF) method with high accuracy on the premise of considering the drift in current and voltage measurement. Under the new European driving cycle (NEDC) test conditions, the advantages of this method are verified[24, 39, 40]. Because of the complex electrochemical reaction during the use of the battery, it often shows strong nonlinear characteristics[41]. The above methods have their own advantages and disadvantages. How to improve the existing methods and make the best trade-off between estimation accuracy and time cost is a problem that researchers are constantly exploring [42].

On the premise of ensuring the accuracy of the model and reducing the calculation cost, the Thevenin equivalent model of lithium-ion battery the second-order RC model are taken as the research object, and the model parameters that best meet the internal characteristics of lithium battery are iteratively calculated by using the improved adaptive particle swarm optimization algorithm, and the accuracy of the model parameters is verified under hybrid pulse power characteristic (HPPC) conditions. Considering the interference caused by the uncertain noise of lithium-ion battery system to SOC estimation, a noise statistical estimator is constructed and combined with extended Kalman iterative algorithm to obtain the real-time SOC value estimated by the minimum variance. The verification results under two different working conditions show that even if the set initial state-of-charge estimation value deviates greatly from the true value, the initial value can still be corrected in a short time to obtain an accurate state-of-charge filter value.

2. MATHEMATICAL ANALYSIS

2.1. Equivalent circuit modeling

At present, the common equivalent circuit models include the internal resistance model, the Thevenin model and PNGV model[1, 43]. The internal resistance model is the most basic equivalent circuit model, but it can't effectively characterize the polarization effect in lithium batteries. The Thevenin model makes up for the defects of the internal resistance model by adding RC circuit based on the internal resistance model. PNGV model considers the change of open circuit voltage caused by the self-discharge effect of lithium li'zi battery, but it also increases the computational complexity accordingly.

Considering the working principle and characteristics of lithium batteries, combining the advantages of common equivalent circuit models, fully considering the internal complex electrochemical reactions in the running process of lithium batteries, through the capacity test, charge and discharge experiment and experimental data analysis of 4.2V/50Ah ternary lithium-ion batteries, considering that the self-discharge rate of lithium batteries has been greatly reduced due to the improvement of the manufacturing process, the Thevenin model with simple structure and good effect is selected to characterize the internal state of lithium-ion batteries, as shown in Figure 1.

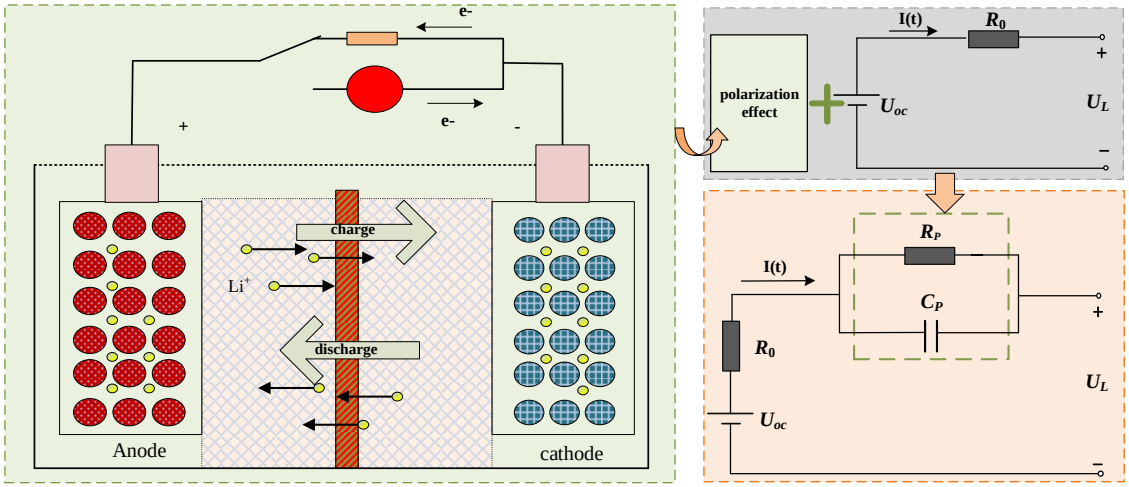

Figure 1. The equivalent circuit model structure

In the figure, U_{oc} represents the open-circuit voltage of lithium battery, and variable resistor R_0 represents the ohmic internal resistance of the lithium-ion battery, and the voltage at both ends is U_0. The parallel circuit composed of R_P and C_P is used to characterize the internal polarization effect of lithium battery, and the voltage at both ends is U_P. According to Kirchhoff's voltage law, the terminal voltage U_L can be expressed as shown in Eq.(1).

$$U_L = U_{oc} - U_0 - U_p \tag{1}$$

According to ohm's law, the relation between U_0, U_P and their current can be listed as shown in Eq.(2)

$$\begin{cases} U_0 = IR_0 \\ U_p(k+1) = -\dfrac{1}{R_P C_P} U_p(k) + \dfrac{1}{C_P} I(k), \end{cases} \tag{2}$$

According to the current-voltage relationship of the Thevenin circuit, the state space equation of the model can be obtained, which provides a theoretical basis for subsequent parameter identification and state estimation model construction.

2.2. Improved adaptive particle swarm optimization algorithm

In order to judge whether the equivalent model of the battery can accurately characterize the working characteristics of the lithium battery, the parameter identification of the equivalent circuit model shouid be carried out first. At present, the commonly used parameter identification methods include the curve fitting method, least square method, KFmethod, etc. The lithium battery is a typical nonlinear system. Considering the limitation of least square method and curve fitting method to nonlinear system, an improved particle swarm optimization algorithm is used to identify circuit parameters.

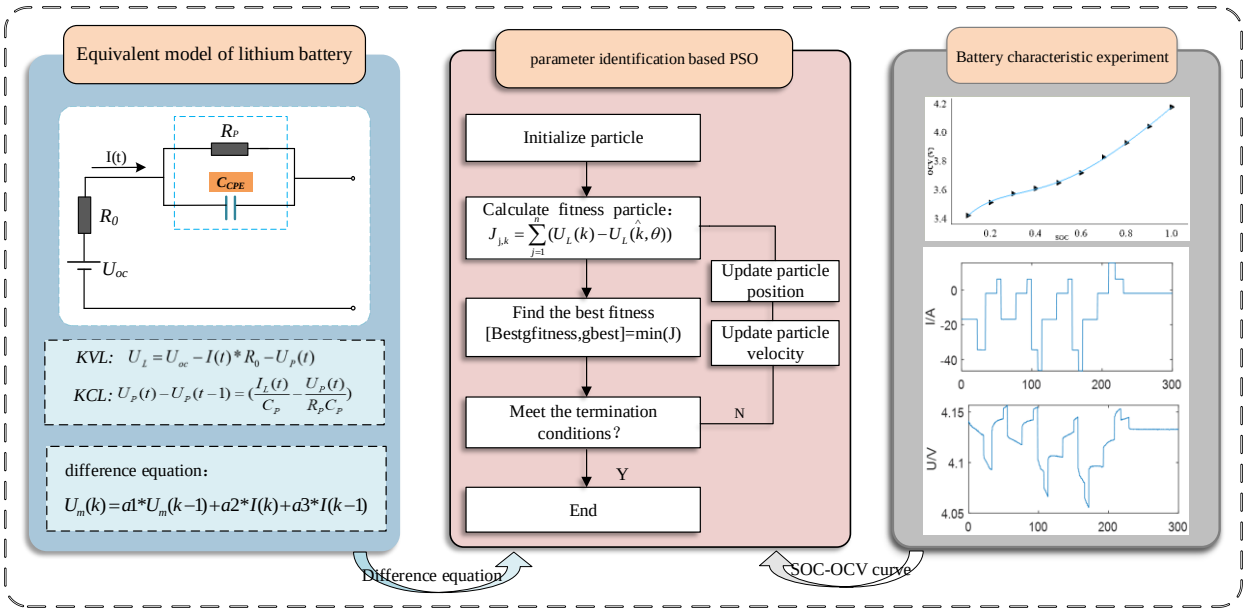

Figure 2. PSO algorithm flow chart

The standard particle swarm optimization algorithm originates from the study of bird predation behavior. The PSO algorithm uses random particles in the M-dimensional solution space as the solution of the problem to be solved, and uses its position to represent. Each particle judges its degree of conformity with the optimal solution through the fitness function. At the same time, the particles update the current position through speed and position transformation. The update of speed and position is not

random, but global search is performed by the globally optimal particles and the individual's historical optimal to converge to the optimal solution. The iterative process of particle swarm optimization algorithm is shown in Figure 2

As shown in Figure 2, the improved particle swarm optimization algorithm is used for parameter identification, and the specific steps are as follows.

Step 1: Let i=0 and initialize a group of particles with dimension m. Each particle represents a possible solution in the solution space. In order to have faster convergence speed and calculation accuracy, it is necessary to set the scope of the solution space and the maximum search speed according to historical experience. Initialize a group of three-dimensional particle swarm according to the number of parameters to be identified, including the number, speed and position setting of particle swarm.

Step 2: Calculate the fitness of particle population at time i. Calculate the fitness of each particle. The fitness function is a standard for judging the advantages and disadvantages of the particle position. In order to make the identified parameters accurately characterize the space state of the lithium battery, the absolute difference between the model output value corresponding to the particle position and the actual output value of the battery is selected as the fitness function j, as shown in Eq.(3).

$$J = \sum_{j=1}^{n} \left(\left| U_m(k) - U_m(\hat{k}, \theta) \right| \right) \tag{3}$$

In the formula, $U_m(k)$ represents the actual output voltage of the lithium ion battery, and $U_m(\hat{k}, \theta)$ represents the model output voltage under the identified parameters.

Step 3: Selecting particles. Selecting the particle pbest_i with the best fitness from the particle swarm at the time t=i, even if j is the local optimal value; Then, from each local optimum in t=1 to t=i, the position gbest_i with the best fitness is selected. Judging whether gbest_i meets the convergence condition, if so, the global search ends, and the identification result is the position corresponding to gbest_i, If not, proceed to the next step.

Step 4: Update the speed and position of particle swarm. The speed update formula and position update formula are shown in Eq.(4).

$$\begin{cases} v_{id}^{k+1} = w * v_{id}^{k} + c1 * \eta_1 * (P_{id}^{k} - x_{id}^{k}) + c2 * \eta_2 * (P_{gd}^{k} - x_{id}^{k}) \\ x_{id}^{k+1} = x_{id}^{k} + \gamma v_{id}^{k+1} \end{cases} \tag{4}$$

Among them, $v_{id}^{k+1}$is the speed at the moment of k+1, ω is the inertia weight coefficient, which generally taken as a value between 0.4 and 0.9. The larger the value of ω, the larger the range of particle search, but the convergence speed will also slow down correspondingly. c1 and c2 are self-cognitive weight coefficient and social cognitive weight coefficient, respectively, and their values determine the following situation of particle position with local optimum and global optimum. $\eta_1$andη_2 are random numbers between (-1,1).

Step 2-Step 4 is carried out cyclically and iteratively, and keeps approaching the optimal value until the convergence condition is reached.

Particle Swarm Optimization (PSO) algorithm is easy to fall into local optimum, so it is considered to improve PSO algorithm with adaptive adjustment strategy to improve the convergence speed and estimation accuracy of the algorithm as a whole. It can be seen from Eq.(4) that the search

speed of particles changes with the value of inertia weight w, and a larger inertia factor is beneficial to jump out of the local minimum and facilitate global search, while a smaller inertia factor is conducive to accurate local search of the current search area to facilitate algorithm convergence; However, if ω is too large, it will easily lead to premature convergence and oscillation near the global optimal solution in the later stage of the algorithm. In order to make a proper trade-off between search speed and accuracy of results, a PSO algorithm based on adaptive weight is established, and an improved PSO algorithm whose inertia weight ωdynamically changes with iteration times and particle position is established. The formula of dynamic change of inertia factor ω is shown in Eq.(5)

$$\begin{cases} w = w_{\min} + \dfrac{(w_{\max} - w_{\min}) * (J - J_{\min})}{J_{avg} - J_{\min}}, J < J_{avg} \\ w = w_{\max}, J > J_{avg} \end{cases} \tag{5}$$

In the formula, J represents the current target function value of particles, and J_{avg} represents the average target value of particles. According to the iteration times of the algorithm and fitness function of particles, the inertia weight ω will increase when the target values of each particle tend to be consistent or local optimum, but decrease when the target values of each particle are scattered. Meanwhile, for particles whose target function value is better than the average target value, the corresponding inertia weight factor is smaller, thus retaining the particle. On the contrary, for particles whose target function value is worse than the average target value, the corresponding inertia weight factor is larger, which makes the particle orientation better.

PSO algorithm is a process of iterative optimization, so it needs the discrete state space equation of lithium battery. According to the current-voltage relationship of equivalent circuit model and Kirchhoff's law, the differential equation is discretized to obtain its difference equation, and its recursion process is shown in Table 1.

Table 1. Difference Equation of Equivalent Circuit Model

Step 1: List the state equation of the model	
Step 2: Discretization of Equation	$\begin{cases} \dfrac{U_p(k) - U_p(k-1)}{T} = -\dfrac{1}{R_p C_p} U_p(k+1) + \dfrac{I}{C_p} \\ U_p(k) = U_{oc} - U_L(k) - I(k) * R \\ U_p(k-1) = U_{oc} - U_L(k-1) - I(k-1) * R \end{cases}$
Step 3: Organize and Simplify	$U_m(k) = \dfrac{R_p C_p}{R_p C_p + T} U_m(k-1) - (\dfrac{TR_p}{R_p C_p + T} + R_0) I(k) + \dfrac{RR_p C_p}{R_p C_p + T} I(k-1)$

Adaptive particle swarm optimization (APSO) algorithm has good advantages in the field of multi-parameter identification. Compared with curve fitting, it has less computation and less hardware requirements, and is suitable for identifying the equivalent model parameters of lithium-ion batteries.

2.3. Extended Kalman filter

As a parameter that can directly evaluate the remaining capacity of lithium batteries, whether SOC can be accurately estimated in real time has become the most important factor affecting the safe and reliable operation of lithium batteries. At present, the SOC estimation method commonly used in the market is generally the Ah method, but the Ah method has accumulated SOC errors that cannot be eliminated, which leads to increasing estimation errors. Considering the strong nonlinear characteristics of lithium-ion batteries, the input and observation data are obtained by designing experiments under actual working conditions, and the state of charge of lithium batteries is iteratively estimated according to extended Kalman filter (EKF) algorithm. In order to improve the adaptability of the equivalent modeling process, the HPPC experimental voltage curve is used to obtain the model parameters that change with the state of charge in real time, so as to realize accurate state of charge estimation. KFalgorithm is an autoregressive algorithm which observes input and output signals on the basis of constructing the state space equation of linear system, corrects the estimated value of the system by denoising the observed value, and iterates continuously to reach the optimal value. EKFsolves the defect that KF algorithm can only be applied to linear systems by Taylor expansion of iterative matrix. The flow chart of KF algorithm is shown in Figure 3.

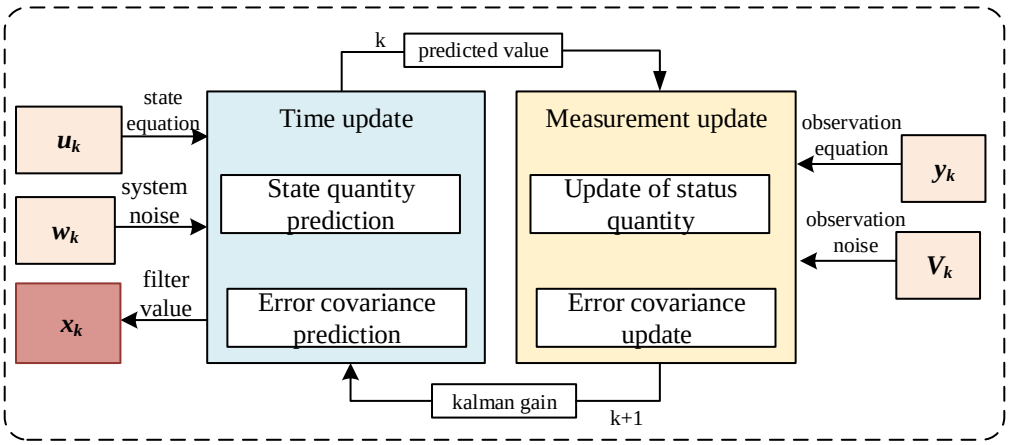

Figure 3. KF algorithm flow chart

As shown in the flow chart, firstly, it is necessary to set boundary conditions for KF algorithm, that is, initialize the state vector x and its error covariance vector p containing the parameter SOC to be estimated. The main part of the algorithm includes five parts: state variable time update, error covariance time update, gain matrix update, state variable measurement update and error covariance measurement update. For linear systems, the best filtering results can be achieved by iterative estimation of the system state vector using KF algorithm. For nonlinear systems, EKF algorithm is needed to linearize the space state equation by Taylor expansion. For a typical nonlinear system, its state equation and observation equation can be expressed as shown in Eq. (6).

$$\begin{cases} x_{k+1} = f(x_k, u_k) + \omega_k \\ y_k = g(x_k, u_k) + v_k \end{cases} \tag{6}$$

Among them, system noise ω_k and observation noise v_k are Gaussian white noises, and their specific definitions are shown in Eq. (7).

$$\begin{cases} E(\omega_k) = 0, \ E[\omega_k \omega_t] = Q_k \delta(k-t) \\ E(v_k) = 0, \ E[v_k v_t] = R\delta_k(k-t) \end{cases} \tag{7}$$

In Eq. (6)., x_k is the state vector, u_k is the input vector, and y_k is the observation vector. $f(x_k, u_k)$ is a nonlinear state equation function of the system, which represents the cumulative change of state quantity under the action of input vector u_k, and $g(x_k, u_k)$ is a nonlinear observation equation function of the system. The nonlinearity of state equation and observation equation will limit the recursive iterative process of KF algorithm, and it is necessary to carry out the first-order Kalman expansion of $f(x_k, u_k)$ and $g(x_k, u_k)$ at each sampling point as shown in Eq. (8).

$$\begin{cases} f(x_k, u_k) = f(\hat{x}_k, u_k) + \dfrac{\partial f(x_k, u_k)}{\partial x_k}\Big|_{x_k = \hat{x}_k} (x_k - \hat{x}_k) \\ g(x_k, u_k) = g(\hat{x}_k, u_k) + \dfrac{\partial g(x_k, u_k)}{\partial x_k}\Big|_{x_k = \hat{x}_k} (x_k - \hat{x}_k) \end{cases} \tag{8}$$

In this formula, $\hat{x}_k$ is the predicted value of the state vector at k time. after linearizing the space state equation, the linear system state equation and observation equation can be obtained as shown in Eq. (9).

$$\begin{cases} x_{k+1} = \hat{A}_k x_k + [f(\hat{x}_k, u_k) - \hat{A}_k x_k] + \omega_k \\ y_k = \hat{C}_k x_k + [g(\hat{x}_k, u_k) - \hat{C}_k x_k] + v_k \end{cases} \tag{9}$$

In this formula, the system matrix $\hat{A}_k$ and the observation matrix $\hat{C}_k$ correspond to the first-order Taylor expansion coefficients of $f(x_k, u_k)$ and $g(x_k, u_k)$, respectively, and the specific form is shown in Eq. (10).

$$\begin{cases} A_k = \dfrac{\partial f(x_k, u_k)}{\partial x_k}\Big|_{x_k = \hat{x}_k} \\ B_k = \dfrac{\partial g(x_k, u_k)}{\partial x_k}\Big|_{x_k = \hat{x}_k} \end{cases} \tag{10}$$

The nonlinear system can be subjected to iterative filtering processing through the linearization processing described above. The specific iterative steps of KF algorithm are as follows.

(1) Initialize state vector and error covariance matrix

$$\hat{x}_{0|0} = E(x_0), \ P_{0|0} = \mathrm{var}(x_0)$$

(2) Time update of state variables

$$\hat{x}_{k|k-1} = A_{k-1}\hat{x}_{k-1|k-1} + B_{k-1}u_{k-1} + q_k$$

(3) Time updating of error covariance

$$P_{k|k\text{-}1} = E[(x_k - \hat{x}_{k|k-1})(x_k - \hat{x}_{k|k-1})^T] = A_{k-1}P_{k\text{-}1|k\text{-}1}{A_{k-1}}^T + Q_{k-1}$$

(4) Update the gain matrix

$$K_k = P_{k|k-1}{C_k}^{\mathrm{T}}(C_k P_{k|k-1}{C_k}^T + R_k)^{-1}$$

(5) Measurement and update of state variables

$$\hat{x}_{k|k} = \hat{x}_{k|k-1} + K_k(y_k - C_k\hat{x}_{k|k-1} - D_k u_k - r_k)$$

(6) updating the error covariance measurement

$$P_{k|k} = (E - K_k C_k)P_{k|k-1}$$

In this formula, $\hat{x}_{0|0}$ and $P_{0|0}$ are the initial values of system state and covariance matrix, $\hat{x}_{k|k-1}$ is the estimated value of state, $\hat{x}_{k|k}$ is the filtered value of state, $P_{k|k-1}$ is the prediction error covariance matrix, $P_{k|k}$ is the filtering error covariance matrix, and K_k is the Kalman gain. After the system is initialized, the filter estimation value of each sampling point is updated twice by KFalgorithm. Time update is to predict the state quantity and error covariance at the previous time according to the filtered value and input quantity at the previous time. The measurement update is based on the observed value outside the system, and the state prediction value and error covariance prediction value under the system noise are considered for correction, so as to obtain the optimal estimation in the sense of minimum variance. The obtained optimal filter value will be used as the input when updating the time at the next moment, so as to realize continuous "prediction-correction" recursive calculation.

2.4. Sage-Husa adaptive filtering

In the traditional SOC estimation model, the system error is the ideal white Gaussian noise. However, in practical engineering applications, the system noise is often very complex and changeable. In order to eliminate the interference caused by the noise error, an adaptive noise statistical estimator based on Sage-Husa algorithm is constructed to adaptively correct the system noise. Combining the adaptive noise statistical estimator with EKF algorithm, Sage-Husa adaptive filtering algorithm is used to constantly modify the process noise covariance and measurement noise covariance in EKF formula, so as to obtain unbiased filtering results under time-varying colored noise. The noise update process based on Sage-Husa algorithm is as follows.

1. Update of process noise value

$$\hat{q}_k = (1-\lambda_k)\hat{q}_{k-1} + \lambda_k(x_k - \hat{x}_{k|k-1})$$

In the formula, $\hat{q}_k$ is the updated value of process noise at k time, and λ_k is the weight based on forgetting factor: $\lambda_k = \frac{1-b}{1-b^k}$, where b is the forgetting factor and the value is 0.95.

2. Covariance update of process noise

$$Q_k = (1-\lambda_k)Q_{k-1} + \lambda_k(K_k(y_k - \hat{y}_{k|})K_k^T)$$

3. Update of measurement noise value

$$\hat{r}_k = (1-\lambda_k)\hat{\lambda}_{k-1} + \lambda_k(y_k - C_k\hat{x}_{k|k-1} - D_k u_k)$$

4. . Covariance update of measurement noise

$$R_k = (1-\lambda_k)R_{k-1} + \lambda_k((y_k - \hat{y}_k)(y_k - \hat{y}_k)^T)$$

Through the above-mentioned four-step filtering calculation, the maximum a posteriori estimation algorithm is used to estimate the system noise, and then the statistical characteristics of the system process noise and observation noise are estimated and corrected in real time while recursive filtering is carried out by using the observation data, so as to achieve the purposes of reducing the model error, restraining the filter divergence and improving the filter accuracy.

2.5. Iterative estimation of state of charge

SOC is an index to measure the remaining battery charge. It is usually defined as the ratio between the charge stored in the battery and the charge that can be stored when fully charged, and it is the most direct reflection of the battery state. Reliable SOC estimation can help Battery management system (BMS) manage energy better, and avoid the phenomena such as greatly shortening the service life of lithium batteries and thermal runaway. Accurate estimation of SOC value is very important to guarantee the working performance of lithium-ion battery. In order to establish a more accurate state of charge estimation model, the ampere-hour integration method and the equivalent model space state description which can accurately characterize the working characteristics of lithium batteries are comprehensively considered. The discrete state space equation of the EKF algorithm is given by the ampere-hour integration process, and the state space description of the equivalent model is embodied in the observation equation of the EKF algorithm, which can be obtained from the KVL relation of the equivalent circuit model, as shown in Eq. (11).

$$\begin{cases} SOC_{k+1} = SOC_k - \dfrac{\eta}{Q_N} I_k \Delta t + \omega_{k1} \\ U_{pk+1} = (1 - \dfrac{\Delta t}{R_P C_P}) \mathrm{U}_{pk} + \dfrac{\Delta t}{C_P} I_k \\ UL_k = f(SOC_k) - I_k R_0 - U_{pk} + \upsilon_k \end{cases} \tag{11}$$

In which, Q_N represents the rated capacity of the battery, I represents the current, where the default discharge point direction is the positive direction, Δt is the sampling time interval, and η represents the charge and discharge efficiency. ω_k stands for process noise, which is Gaussian white noise with a mean value of 0 and a variance of Q, and represents the internal error distribution during the system operation. U_L is terminal voltage, f(soc) is open circuit voltage, which is a nonlinear function of SOC, SOC represents open circuit voltage, R_0 and R_P represent ohmic resistance and polarization resistance in equivalent circuit model respectively, τ is time constant of RC circuit, v_k is observation noise, white Gaussian noise with mean value of 0 and variance of R, which represents error distribution during observation. Selecting the state vector as $\mathrm{X} = [SOC \quad U_P]$, according to the KVL relation of the equivalent circuit model, the discrete space state equation can be obtained, as shown in Eq. (12)

$$\begin{cases} X_{k+1} = AX_k + Bu_k + \begin{bmatrix} w_{1,k-1} \\ w_{2,k-1} \end{bmatrix}, X = \begin{bmatrix} SOC_k \\ U_{p,k} \end{bmatrix} \\ U_{L,k} = U_{oc,k} - R_{0,k} I_k + \begin{bmatrix} 0 \\ -1 \end{bmatrix}^T \begin{bmatrix} SOC_k \\ U_{p,k} \end{bmatrix} + v_k \end{cases} \tag{12}$$

Among them, the meanings of state transition matrix A and input matrix B come from the process recursion equation, which is the driving matrix for obtaining the state of the next moment from the state of the previous moment, which can be obtained from the space state equation of Eq. (11). C is the observation matrix. Because the measurement equation is nonlinear, it is necessary to carry out Taylor expansion on the measurement equation, and the coefficient of the obtained state variable is the value of C. and the specific forms of A , B and C are shown in Eq.(13).

$$A=\begin{bmatrix}1 & 0\\ 0 & 1-\dfrac{\Delta t}{R_pC_P}\end{bmatrix},\ B=\begin{bmatrix}-\dfrac{\eta\Delta t}{Q_n}\\ \dfrac{\Delta t}{C_p}\end{bmatrix},C=\begin{bmatrix}\dfrac{\partial f(SOC)}{\partial(SOC)} & 0\end{bmatrix} \tag{13}$$

Because the EKF algorithm omits the higher order term of Taylor expansion in the estimation process, and the noise is artificially defined as Gaussian white noise in the estimation process, it may lead to the problem of filtering divergence in the estimation process. In order to achieve the best filtering effect, an adaptive adjustment factor is considered to correct the error based on the extended Kalman algorithm.

3. RESULTS AND DISCUSSION

3.1. Experimental platform design

In order to verify the accuracy of the model parameters and the tracking of the filtered results of the SOCand the true values, an experimental platform for lithium batteries was built, and relevant experiments were designed according to the actual working conditions to obtain experimental data. The experimental platform and the parameters of lithium-ion battery used in the experiment are shown in Figure 4.

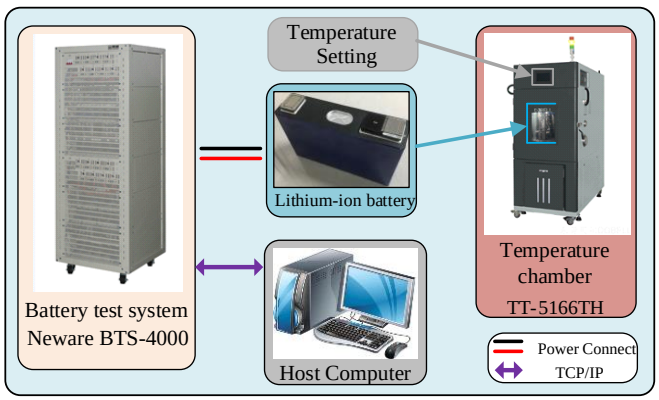

Parameters of lithium ion battery

Lithium-ion battery type	ternary lithium-ion battery
Rated capacity	50Ah
nominal voltage	3.7V
Maximum sustained discharge rate	3C
Battery weight	850g
Upper charging limit voltage	4.2V
Lower charging limit voltage	2.75V

Figure 4. experimental equipment

As shown in Figure 4, the lithium battery used in this experiment is a ternary lithium-ion battery with a nominal capacity of 50Ah and a charging voltage of 4.2V. The temperature control test box TT-5166TH can provide a constant temperature environment when the battery is charged and discharged. Neware BTS-4000 is a high-power charge and discharge tester for power batteries, which is used for charging and discharging lithium batteries. The charging and discharging of lithium battery is connected to the master computer of the charging and discharging tester, and the charging and discharging steps

are set by the maste computer. Through such a man-machine interaction module, the working condition experiment of lithium battery in constant temperature environment can be controlled.

3.2. Working characteristics of lithium battery

There are two main characteristics that related to SOC estimation of lithium-ion battery: the one is Charging and discharging characteristic, the other one is OCV characteristic.

In order to explore the changes of internal characteristics of lithium-ion batteries at different charging and discharging rates, the lithium-ion batteries were charged to the cutoff current in a constant current and constant voltage mode, and then discharged to the cutoff voltage of 2.75V at the rates of 0.5c, 0.8c, 1c and 1.5c respectively. The voltage variation curves and output capacity curves under different rate discharge experiments are shown in Figure 5.

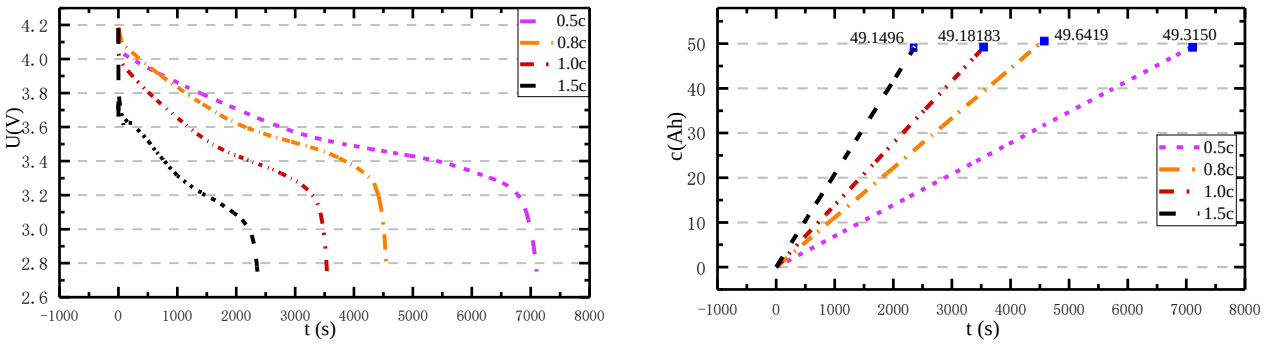

(a) Voltage curve (b) capacity curve

Figure 5. Discharge curves at different rates

It can be seen from Figure 5 that as the discharge speed of the battery increases, the voltage drops faster, and the discharged capacity of the battery also decreases. The open-circuit voltage is the terminal voltage of lithium-ion battery when it is at rest for a long time. In the static state, the OCV and the state of charge of lithium ion batteries have a good mapping relationship. Open-circuit voltage characteristics of lithium ion voltage are studied to determine the one-to-one correspondence between OCV and state of charge.

The OCV-SOC calibration experiment of lithium-ion battery is carried out using battery testing equipment with set time. In this experiment, the battery is intermittently discharged at a discharge rate of 1 C. The discharge time for each cycle is set according to the set discharge rate and the number of required relationship coordinate points. In this experiment, 10 relationship coordinate points are needed, so each discharge time is 6 minutes. The last discharge experiment will probably not last until the expected discharge time, and the discharged capacity can be obtained according to the discharge duration and the discharge current, thus obtaining the SOC of the battery after the last discharge. After each discharge, the battery is put aside for 1h to stabilize its internal chemical state to obtain its open circuit

voltage. As shown in Figure 6, these discrete points are extracted from laboratory data to obtain the OCV-SOC relationship scatter diagram, and the least square method is used to fit to obtain the OCV-SOC relationship curve and relationship polynomial.

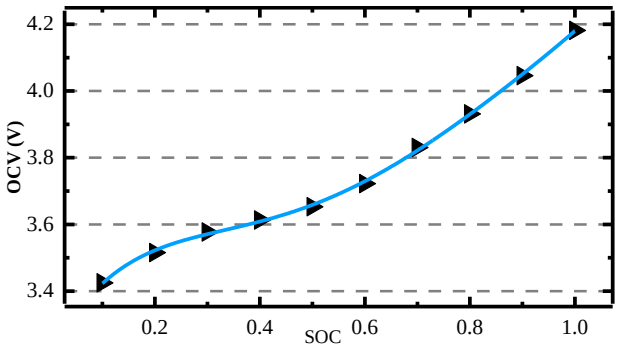

Figure 6. OCV-SOC fitting curve

Scatter points obtained from experiments are points with high trust, so the curve should pass through every point as far as possible, and the curve should accurately reflect the trend of the relationship between OCV and SOC as far as possible. Therefore, the fitting curve should be smoothly transitioned in the interval between scatter points as far as possible, and the change rate should not be too large. Obviously, the higher the order of the fitting polynomial, the better the fitting accuracy. However, the limit of the processor's operation ability under actual conditions should also be considered, that is, the fitting polynomial should not be too high to reduce the computational complexity. Considering the above situation, after repeated tests and comparison of fitting results, it is finally found that the fitting effect of 5th order polynomial is better, and the complexity is moderate and acceptable for the processor. Therefore, the function relation of OCV-SOC obtained by fitting with a 5-order polynomial is shown in Eq. (14).

$$UOC = 4.277 \times SOC^5 - 14.71 \times SOC^4 + 18.98 \times SOC^3 - 10.63 \times SOC^2 + 3.039 \times SOC + 3.216 \quad (14)$$

3.3. Parameter identification

In the designed circuit model, the parameters to be identified include $\theta = [R_0, R_p, C_p]$. APSO algorithm is used to identify the model parameters. Parameters R0, Rp, Cp to be identified are represented by three-dimensional particles $\theta = [R_0 \quad R_p \quad C_p]$, which have two attributes: position and velocity. Design a particle population with 20 particles. In each iteration process, each particle needs to update its position and velocity, judge the output voltage error corresponding to the particle position, record the particle position pbest_i corresponding to the minimum error in each iteration and the optimal position gbest_i in all time series, and update the position and velocity of each particle according to these two positions until the convergence condition is reached. The battery is tested under Beijing bus dynamic

stress test (BBDST) condition, and the real-time current and voltage data are collected as the estimation basis of APSO. The identified model parameters and errors are shown in Figure 7.

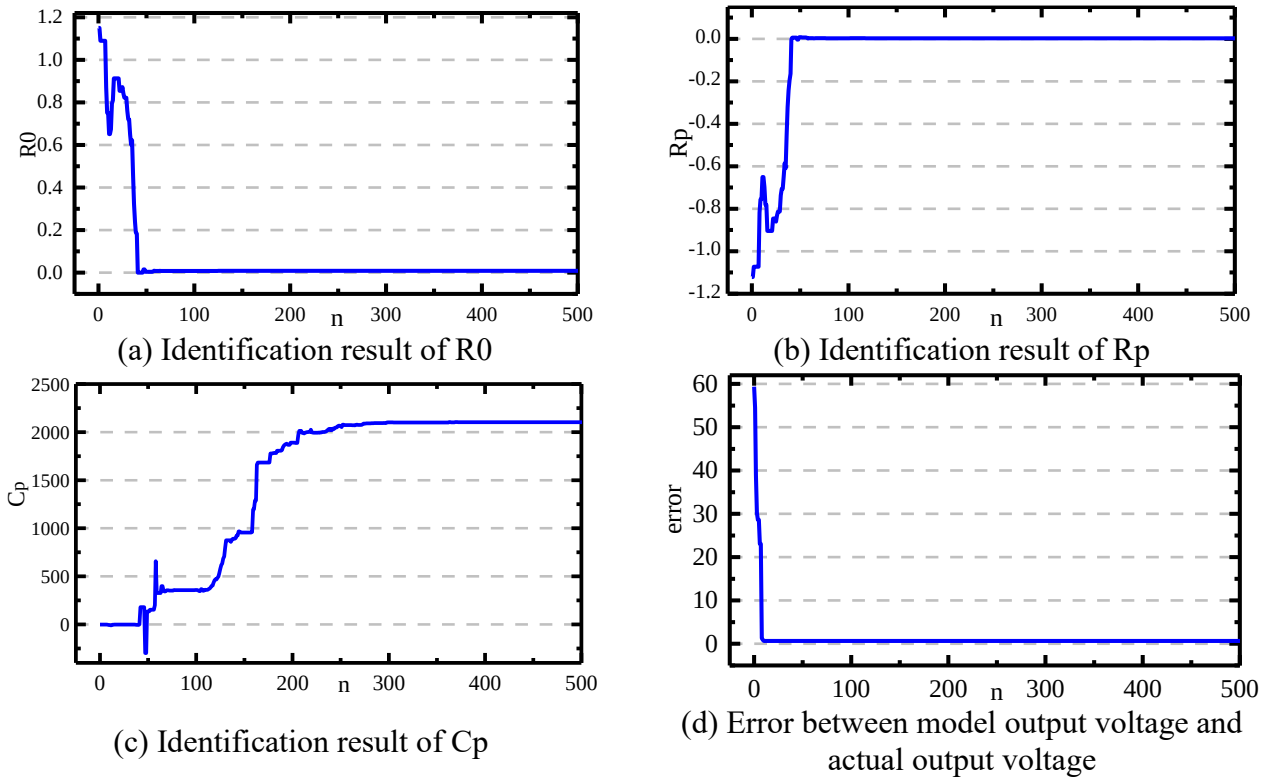

Figure 7. Parameter Identification Results

It can be seen from the figure that the APSO algorithm can quickly iterate to obtain the optimal model parameters, and the adaptive method can greatly avoid local convergence and improve the credibility of the identification results. The specific identification results are shown in Table 2.

Table 2. Parameter Identification Results

R_0/Ω	Rp/Ω	Cp/F
0.001954	0.000572	2098.71

After the identification results are obtained, they are used as the input parameters of the state-of-charge estimation model to provide data support for state estimation.

3.4. Modelling verification

After obtaining the mathematical description of each parameter of the model, it is necessary to verify the accuracy of the model parameters. Put the identified parameters into the equivalent circuit

model, input the same current change as the HPPC test experiment, compare the output voltage response of the model with the actual voltage data, verify the model, and optimize and improve the model according to the verification results. The verification result of model parameters is shown in. Figure 8.

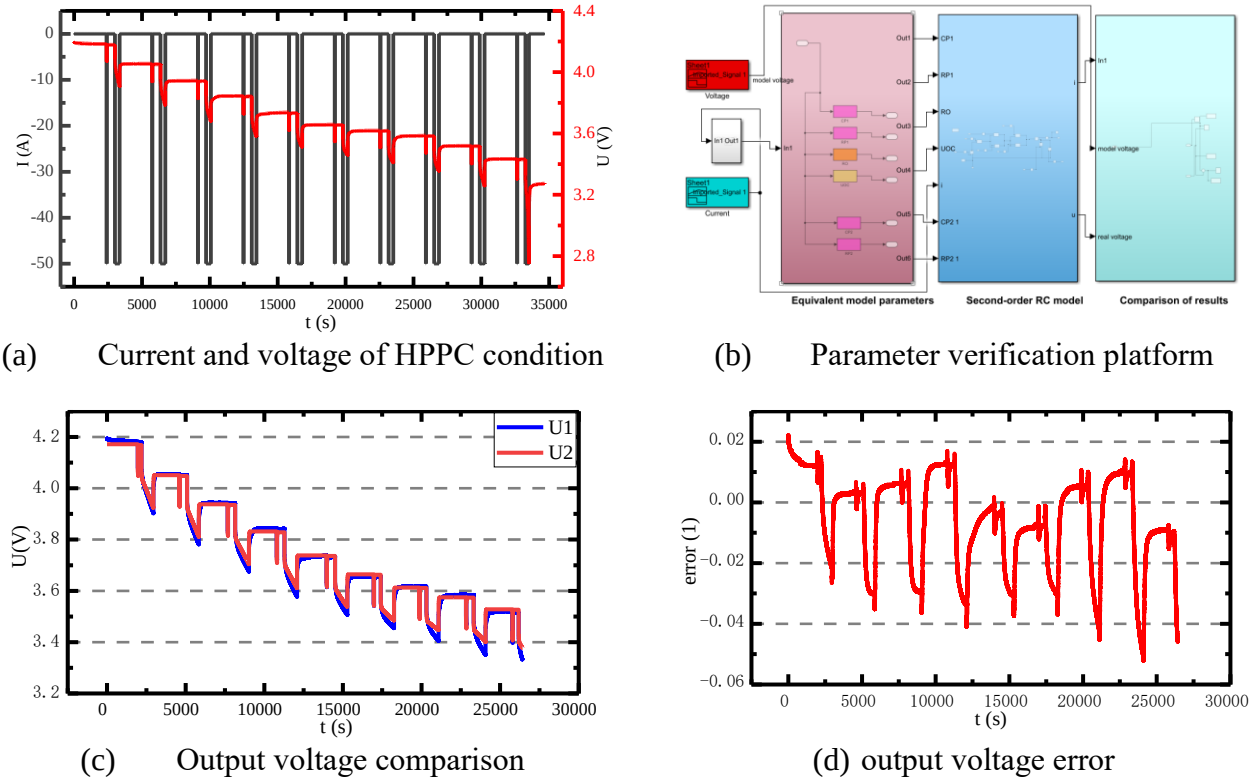

(a) Current and voltage of HPPC condition (b) Parameter verification platform

(c) Output voltage comparison (d) output voltage error

Figure 8. Verification results of Thevenin model parameters

As shown in the above figure, Figure 8(a) shows the input current and output voltage of HPPC working condition, and Figure 9(b) shows the built parameter verification platform, which includes an experimental data input module for simulated working condition, an equivalent circuit model and parameter input module, and a model output and actual output comparison module. Through this verification platform, the curve comparison between the model output voltage and the actual output voltage and the absolute error curve can be obtained.

As shown in Figure 8 (c), the red curve is the model output terminal voltage, and the blue curve is the actual battery output terminal voltage. it can be seen that the model output terminal voltage is in good agreement with the actual value, which explains the rationality of the Thevenin equivalent circuit model and also proves the feasibility and reliability of the parameter identification method.

From the error curve in Figure 8(d), it can be seen that the model did not diverge during the whole process, and the larger error occurred at the power pulse test stage, because the sudden change of battery input current caused the accumulation of chemical reactions inside the battery to increase, resulting in a rapid change of terminal voltage. Even in the last stage when SOC is very low and the model cannot well reflect the current state of the battery, the maximum error does not exceed 0.06V.

In order to verify the parameter estimation effect of APSO algorithm for different models, the second-order RC equivalent circuit model is identified by the same method, and the model parameters are used to verify the coincidence between the output voltage of the model and the actual output voltage[3, 14, 40, 44]. The verification effect under the parameters of the second-order equivalent circuit model is shown in Figure 9.

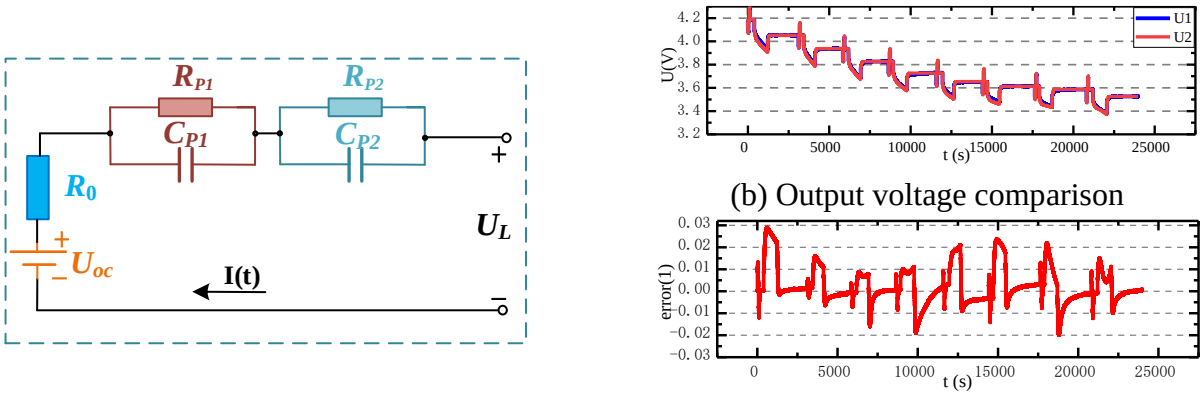

(a) Second-order RC model

(b) Output voltage comparison

(c) Output voltage error

Figure 9. Parameter verification results of second-order RC model

Figure 9(a) is a second-order equivalent circuit model, and Figure. (b) and (c) are the comparison curves of actual output voltage and model output voltage and absolute error curves of the second-order RC equivalent model under HPPC operating conditions, where U1 is the output voltage under actual operating conditions and U2 is the model output voltage of the second-order RC equivalent model under the same operating conditions.

It can be seen from the Figure 9 that when identifying the equivalent circuit model parameters with higher accuracy, the model parameters identified by the APSO algorithm have a higher matching degree with the internal characteristics of the lithium ion battery. The average error of the model identified by the same algorithm is less than 0.0025, the maximum output error is less than 0.03, and the algorithm accuracy is greater than 99.3%. It is proved that the adaptive particle swarm optimization algorithm has high accuracy and robustness in identifying the parameters of lithium ion battery model.

3.5. Simulation and verification of algorithms

In order to verify the robustness of AEKF algorithm under complex working conditions, 50Ah/4.2V lithium iron phosphate battery was tested with reference to various working conditions experiments[9, 43]. The hybrid pulse test experiment was carried out at a constant temperature of 25℃, and the input current signal and voltage observation signal under the influence of noise were obtained. The verified real state is based on the Ahintegral measurement with the minimum time interval added with adaptive noise, and the complicated and changeable colored noise is added as interference, which is used as a comparison to check the state output effect under different working conditions. The actual

operating conditions are simulated by data, and the effective number of data is redefined in Matlab environment for processing, so as to obey the normal distribution of random noise, that is, Gaussian white noise with a mean value of zero and a variance of R, which is superimposed on the input data to simulate the actual observed terminal voltage. This data is used as the terminal voltage comparison for updating the state of charge estimation. Input current and observed voltage under simulated noise are predicted and updated by AEKF algorithm based on improved equivalent circuit model, and the estimated value of output SOC is obtained[45]. Meanwhile, in order to simulate the interference to the estimation model when the initial value is unknown, the initial value of SOC is designed to be 0.85. The simulation results of the algorithm under HPPC condition are shown in Figure 10(a) and (b), and the verification results under BBDST condition are shown in Figure. 10(c) and 10(d), where SOC1 is the reference value of state of charge, SOC2 and error1 are the estimation result and error based on EKF algorithm respectively, SOC3 and error2 are the estimation result and error based on AEKF respectively.

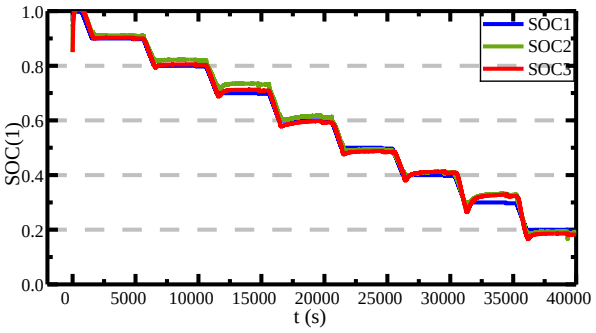

(a) SOC estimation result under HPPC experiment

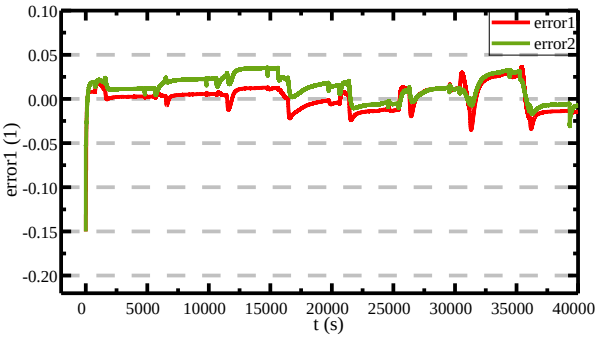

(b) error of soc estimation under HPPC experiment

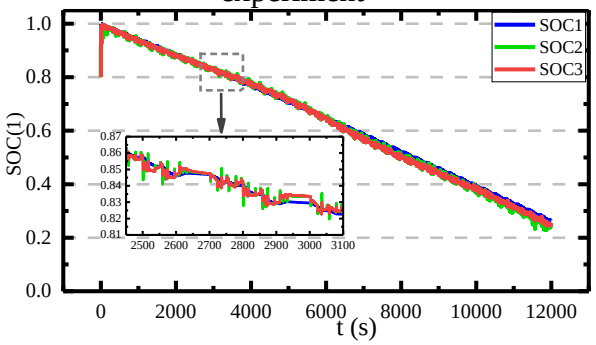

(c) SOC estimation result under BBDST test

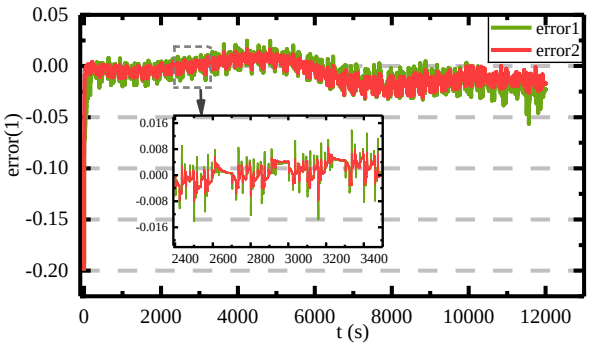

(d) error of soc estimation under BBDST test

Figure 10. SOC estimation results under different test conditions

It can be seen from the estimation results of Figure 10 under two working conditions that the algorithm can converge to the real value at a very fast speed even when the initial value of SOC deviates greatly from the real value. Compared with EKF algorithm, AEKF algorithm achieves higher estimation accuracy by correcting noise interference. Through the analysis of the output results, it can be concluded that when the initial value is wrong, the AEKF algorithm has the ability of noise adaptive and automatic adjustment. The maximum estimation error under the whole HPPC working condition is not more than 0.04, and the estimation error under BBDST is less than 0.06, which shows good stability and robustness.

4. CONCLUSIONS

Effective equivalent modeling and accurate state of charge estimation are the key technologies of BMS. In order to better monitor the state of battery pack, based on the experimental study of the ternary lithium-ion battery, taking the Thevenin equivalent model as the object, APSO algorithm is innovatively introduced to realize the parameter identification of the model. The simulation results show that the maximum deviation between the simulation value and the actual terminal voltage is less than 0.06 volts, and the model accuracy can reach more than 98%. On the basis of experimental research and accurate battery parameter identification, the AEKFalgorithm is used to estimate the state of charge. The algorithm verification results under two different working conditions show that the algorithm has good adaptability and robustness. Even when the initial state-of-charge value deviates, the actual state-of-charge value can be recovered and tracked quickly within 50 seconds, thus realizing accurate estimation of the SOC of lithium-ion batteries. This method provides a reliable basis for SOCestimation under complex colored noise interference.

ACKNOWLEDGEMENTS
The work was supported by National Natural Science Foundation of China (No. 61801407)，Sichuan Science and Technology Department Key RESEARCH and Development Projects (2018GZ0390, 2019YFG0427), the Scientific Research Project of Education Department of Sichuan Province (17ZB0453), Natural Science Foundation of Southwest University of Science and Technology (No.17zx7110, 18zx7145).

References

1. D. W. He, W. Zhang and X. Y. Luo, *IOP Conference Series: Earth and Environmental Science*, 461 (2020) 012032.
2. H. He, X. Zhang, R. Xiong, Y. Xu and H. Guo, *Energy*, 39 (2012) 310.
3. N. Zhang, Y. Zhou, Q. Tian, X. Liao and F. Zhang, *International Journal of Precision Engineering and Manufacturing*, 20 (2019) 845.
4. X. Liu, W. Li and A. Zhou, *IEEE Access*, 6 (2018) 23639.
5. C. Lin, Q. Yu, R. Xiong and L. Y. Wang, *Applied Energy*, 205 (2017) 892.
6. R. Xiao, J. Shen, X. Li, W. Yan, E. Pan and Z. Chen, *Energies*, 9 (2016) 184.
7. Y. Zhang, R. Xiong, H. He and M. G. Pecht, *IEEE Transactions on Vehicular Technology*, 67 (2018) 5695.
8. J. Rivera-Barrera, N. Muñoz-Galeano and H. Sarmiento-Maldonado, *Electronics*, 6 (2017) 102.
9. W. Zhao, X. Kong and C. Wang, *Proceedings of the Institution of Mechanical Engineers, Part D: Journal of Automobile Engineering*, 232 (2017) 357.
10. R. Zhang, J. Wu, R. Wang, R. Yan, Y. Zhu and X. He, *IEEE Transactions on Industrial Electronics*, 66 (2019) 5979.
11. C. Zhang, W. Allafi, Q. Dinh, P. Ascencio and J. Marco, *Energy*, 142 (2018) 678.
12. S. Wang, C. Fernandez, Y. Fan, J. Feng, C. Yu, K. Huang and W. Xie, *Energy Science & Engineering*, 8 (2020) 1484.
13. Y. Qiu, X. Li, W. Chen, Z. M. Duan and L. Yu, *ISA Trans*, 94 (2019) 326.
14. Y. Zheng, W. Gao, M. Ouyang, L. Lu, L. Zhou and X. Han, *Journal of Power Sources*, 383 (2018) 50.
15. P. Vijay and M. O. Tadé, *Computers & Chemical Engineering*, 102 (2017) 2.

16. H. Mu, R. Xiong, H. Zheng, Y. Chang and Z. Chen, *Applied Energy*, 207 (2017) 384.
17. S. Orcioni, L. Buccolini, A. Ricci and M. Conti, *Energies*, 10 (2017) 375.
18. Z. Chen, H. Sun, G. Dong, J. Wei and J. Wu, *Journal of Power Sources*, 414 (2019) 158.
19. Y. Chen, G. Yang, X. Liu and Z. He, *Energies*, 12 (2019) 1803.
20. A. R. Mandli, A. Kaushik, R. S. Patil, A. Naha, K. S. Hariharan, S. M. Kolake, S. Han and W. Choi, *International Journal of Energy Research*, 43 (2019) 2044.
21. M. Luo, Y. Guo, J. Kang, L. She and Z. Geng, *Ionics*, 24 (2018) 1907.
22. A. Barai, K. Uddin, W. D. Widanage, A. McGordon and P. Jennings, *Sci Rep*, 8 (2018) 21.
23. G. Dong, J. Wei, C. Zhang and Z. Chen, *Applied Energy*, 162 (2016) 163.
24. M. Mathew, S. Janhunen, M. Rashid, F. Long and M. Fowler, *Energies*, 11 (2018) 1490.
25. L. H. Zhao, Z. Y. Liu and G. H. Ji, *Control Eng Pract*, 81 (2018) 114.
26. Z. L. Zhang, X. Cheng, Z. Y. Lu and D. J. Gu, *Ieee T Power Electr*, 33 (2018) 2216.
27. S. Wang, C. Fernandez, X. Liu, J. Su and Y. Xie, *Measurement and Control*, 51 (2018) 125.
28. S. Wang, D.-I. Stroe, C. Fernandez, C. Yu, C. Zou and X. Li, *Journal of Power Sources*, 450 (2020) 227652.
29. S. L. Wang, C. Fernandez, Z. W. Xie, X. X. Li, C. Y. Zou and Q. Li, *Energy Science & Engineering*, 7 (2019) 3038.
30. R. Xiong, Y. Zhang, H. He, X. Zhou and M. G. Pecht, *IEEE Transactions on Industrial Electronics*, 65 (2018) 1526.
31. J. Wang, L. Zhang, D. Xu, P. Zhang and G. Zhang, *Mathematical Problems in Engineering*, 2019 (2019) 1.
32. P. Shen, M. Ouyang, L. Lu, J. Li and X. Feng, *IEEE Transactions on Vehicular Technology*, 67 (2018) 92.
33. R. Xiong, Y. Zhang, J. Wang, H. He, S. Peng and M. Pecht, *IEEE Transactions on Vehicular Technology*, 68 (2019) 4110.
34. C. Chen, R. Xiong and W. Shen, *IEEE Transactions on Power Electronics*, 33 (2018) 332.
35. X. Ma, D. Qiu, Q. Tao and D. Zhu, *Applied Sciences*, 9 (2019) 2765.
36. T. Mesbahi, N. Rizoug, P. Bartholomeus, R. Sadoun, F. Khenfri and P. Le Moigne, *IEEE Transactions on Industrial Electronics*, 65 (2018) 1298.
37. M. Dubarry, G. Baure, C. Pastor-Fernández, T. F. Yu, W. D. Widanage and J. Marco, *Journal of Energy Storage*, 21 (2019) 172.
38. Y. H. Chiang, W. Y. Sean and S. M. Jeong, *Journal of Cleaner Production*, 220 (2019) 945.
39. Z. Liu, Z. Li, J. Zhang, L. Su and H. Ge, *Energies*, 12 (2019) 757.
40. J. Meng, D.-I. Stroe, M. Ricco, G. Luo and R. Teodorescu, *IEEE Transactions on Industrial Electronics*, 66 (2019) 7717.
41. T. Bruen and J. Marco, *J Power Sources*, 310 (2016) 91.
42. D. Liu, L. Li, Y. Song, L. Wu and Y. Peng, *International Journal of Electrical Power & Energy Systems*, 110 (2019) 48.
43. *Energies*, 11 (2018) 59.
44. L. Zhao, Z. Liu and G. Ji, *Control Engineering Practice*, 81 (2018) 114.
45. Q. Wang, X. Feng, B. Zhang, T. Gao and Y. Yang, *Journal of Renewable and Sustainable Energy*, 11 (2019) 014302.